The Ohio State University RResearch

The following report from Ohihio State University for the period April-June 1997 is provided below. It contains

Highlights
Dynamic Gas Disengagemennt (Bed Collapse) Technique
References

INTRINSIC FLOW BEHAVIOR IN A SLURRY BUBBLE COLUMN UNDER HIGH PRESSURE AND HIGH TEMPERATURE CONDITIONS

(Reporting Period: April 1 to June 30, 1997)

Highlights

1. The differential pressure signals during bed collapse processes have been converted to the variation of gas holdup with time. From the variation of gas holdup with time, bubbles are divided into five groups based on bubble size. The bubble rise velocity and initial gas holdup in each group are obtained.

2. A reliable correlation for bubble rise velocity is essential to the dynamic gas disengagement technique. A correlation has been developed to calculate the rise velocity of single bubbles in the high-pressure and high-temperature slurry bubble column. Predictions of the correlation are satisfactory.

Dynamic Gas Disengagement (Bed Collapse) Technique

Dynamic Gas Disengagement (DGD) or bed collapse technique offers a simple way to estimate the bubble size distribution in our high-pressure and high-temperature slurry bubble column. The experimental setup for the bed collapse technique and a typical response were described in the January-March 1997 quarterly report.

The differential pressure signal during a complete DGD process is divided into six stages, as described in the January-March 1997 report. (1) Immediately following the gas shutoff is a sudden jump in the differential pressure signal, which corresponds to the simultaneous escape of large and small bubbles. (2) In the second stage, the increase in the signal value is much more gradual, since only small bubbles escape from the bed. (3) The differential pressure remains at a relatively constant value for about 150 seconds because the particles are still fully suspended by the liquid motion induced by bubbles. The first three stages can be analyzed to evaluate the bubble size and bubble size distribution. In the last quarter, experiments were conducted to obtain differential pressure signals during bed collapse processes at zero liquid velocity and various gas velocities ranging from 5.2 to 32.4 cm/s. Figure 1 shows the differential pressure signals of the first three stages under five gas velocity conditions.

To evaluate the bubble size and bubble size distribution, the differential pressure signal should be converted into the variation of gas holdup with time. It can be seen from Figure 1 that the differential pressure signals in stage 3 have the same value of about 2950 Pa/m over the entire gas velocity range, which implies that the catalyst particles are uniformly distributed in the slurry bubble column under the conditions of this work. Based on this observation, it can be assumed that the particles are uniformly distributed in the column, and therefore the ratio of liquid holdup to solids holdup is a constant, K, during the first three stages. K can be calculated from the signal at stage 3, i.e., the gas-free liquid-solid suspension. The differential pressure drop at this stage can be related to the gas-free liquid and solids holdups by the following equation:

$$\left(\frac{\Delta P}{\Delta z}\right)_d^0 = \left(\rho_l\varepsilon_l^0 + \rho_s\varepsilon_s^0 - \rho_l\right) g = \varepsilon_s^0(\rho_s - \rho_l) g \tag{1}$$

Solving Eq. (1) gives the solids holdup in the gas-free liquid-solid suspension:

$$\varepsilon_s^0 = \frac{\left(\frac{\Delta P}{\Delta z}\right)_d}{(\rho_s - \rho_l) g} \tag{2}$$

K can then be written as

$$K = \frac{\varepsilon_s^0}{\varepsilon_l^0} = \frac{\varepsilon_s^0}{1-\varepsilon_s^0} = \frac{(\Delta P/\Delta z)_d}{(\rho_s - \rho_l) g - (\Delta P/\Delta z)_d} \tag{3}$$

With K known, the differential pressure signal can be related to the variation of gas holdup with time during the dynamic gas disengagement process (stages 1 and 2), based on the following equation:

$$\begin{aligned}\left(\frac{\Delta P}{\Delta z}\right)_d &= \left(\rho_g\varepsilon_g + \rho_l\varepsilon_l + \rho_s\varepsilon_s - \rho_l\right) g \\ &= \left\{\frac{K(\rho_s - \rho_l)}{1+K} + \left[\frac{(1+K)\rho_g - (\rho_l + K\rho_s)}{1+K}\right]\varepsilon_g\right\} g\end{aligned} \tag{4}$$

Solving Eq.(4) yields the gas holdup, ε_g:

$$\varepsilon_g = \frac{(1+K)\left(\frac{\Delta P}{\Delta z}\right)_d / g - K(\rho_s - \rho_l)}{(1+K)\rho_g - (\rho_l + K\rho_s)} \tag{5}$$

Figure 2 shows the variations in gas holdup with time through the first three stages at various gas velocities.

The escape of bubbles from the slurry bubble column leads to the gas holdup variation during a bed collapse process. At any moment, bubbles of different sizes emerge simultaneously from the bed surface. Smaller bubbles have lower rise velocities and thus, stay in the bed for a longer period. During the bed collapse process, the slope of an ε_g vs.

t curve keeps decreasing because the bubble size inside the bed becomes smaller, as does the volumetric flow rate of bubbles escaping from the bed surface.

Assume that the bubbles are divided into N size groups, i.e., $d_{B,1}$, ……, $d_{B,N-1}$, $d_{B,N}$, $d_{B,N}$ corresponding to the smallest bubbles. The ε_g vs. t signal can be approximated with N linear segments, designated as $(t_0, \varepsilon_{g,0})$, $(t_1, \varepsilon_{g,1})$, ……, $(t_N, \varepsilon_{g,N})$, shown in Figure 3. The change in slope implies the depletion of a group of bubbles. The decrease in gas holdup between t_{i-1} and t_i is due to the escape of the bubbles smaller than $d_{B,i}$. Therefore, the rise velocity ($U_{b,i}$) and holdup of bubbles of size $d_{B,i}$ ($\varepsilon_{g0,i}$) can be determined by the following equations (Daly *et al.*, 1992):

$$\begin{cases} U_{b,i} = \dfrac{H}{t_i - t_0} \\ \varepsilon_{g0,i} = \dfrac{-\left(HS_i + \sum\limits_{j=i+1}^{N} U_{b,j}\varepsilon_{g0,j} \right)}{U_{b,i}} \end{cases} \qquad i = N, N-1, \ldots, 1 \tag{6}$$

where H is the distance between the gas distributor and the top pressure port and S_i is the slope of the ith segment of curve. Note that calculations by Eq. (6) start from the smallest bubbles and end with the largest bubbles. Table 1 shows the results. With the initial gas holdup of each bubble group and the size of the bubbles, the number of bubbles in each group can be expressed as

$$n_{b,i} = \frac{AH\varepsilon_{g0,i}}{\dfrac{\pi}{6} d_{b,i}^3} \tag{7}$$

A reliable and accurate correlation for the bubble rise velocity is the key to evaluating bubble size using the dynamic gas disengagement technique. The bubble rise velocity in a slurry bubble column is different from that of single bubbles, due to the interaction between bubbles and between bubbles and their surrounding medium. Correlations for bubble swarm rise velocity have been proposed in the literature (Peebles and Garber, 1953; Marrucci, 1965; Clift et al., 1978; Abou-el-Hassan, 1983). Most of the correlations were established on the basis of single-bubble rise velocity. Unfortunately, no reliable correlation is yet available to predict the rise velocity of single bubbles under high-pressure conditions. In this quarter, experiments were conducted to develop a correlation for single-bubble rise velocity that could be applicable under high-pressure and high-temperature conditions. The following correlation (Fan and Tsuchiya, 1990) has been extended to such conditions:

$$U_b' = \left\{ \left[\frac{Mo^{-1/4}}{K_b} \left(\frac{\Delta\rho}{\rho_m} \right)^{5/4} d_e'^{2} \right]^{-n} + \left[\frac{2c}{d_e'} + \left(\frac{\Delta\rho}{\rho_m} \right) \frac{d_e'}{2} \right]^{-n/2} \right\}^{-1/n} \tag{8}$$

where

$$U_b' = U_b(\rho_m/\sigma g)^{1/4}, \qquad d_e' = d_e(\rho_m g/\sigma)^{1/2} \tag{9}$$

and $Mo = g\Delta\rho\mu_m^4/(\rho_m^2\sigma^3)$ with $\Delta\rho = \rho_m - \rho_g$. ρ_m and μ_m are the effective density and viscosity of the liquid-solid medium, respectively. Three empirical constants in Eq. (8), n, c and K_b, reflect the separate factors governing the rate of bubble rise. In the practical use of Eq. (8), n ranges from 0.8 (for contaminated liquids) to 1.6 (for purified liquids); c = 1.2 and 1.4 for monocomponent and multicomponent liquids, respectively; and

$$K_b = \max(K_{b0}\, Mo^{-0.038},\ 12) \tag{10}$$

where K_{b0} = 14.7 and 10.2 for aqueous solutions and organic solvents/mixtures, respectively. The effective viscosity of liquid-solid suspensions is calculated by the following equation:

$$\frac{\mu_m}{\mu_l} = \exp\left[\frac{K\varepsilon_s}{1-(\varepsilon_s/\varepsilon_{sc})}\right] \tag{11}$$

with two parameters correlated by

$$K = \{3.1 - 1.4\tanh[0.3(10 - 10^2 U_t)]\}/\phi \tag{12a}$$

$$\varepsilon_{sc} = \{1.3 - 0.1\tanh[0.5(10 - 10^2 U_t)]\}\varepsilon_s \tag{12b}$$

where U_t is the particle terminal velocity in liquid (m/s), ε_s is the solids holdup at the incipient fluidization/packed state, and ϕ is the shape factor of the particles. Figure 4 compares the experimental data with the predictions of Eqs. (8)-(12). The particles in the experiments were 210-μm glass beads. It can be seen that the correlation proposed here can be used under the experimental conditions of this work. Equations (8)-(12) can then be used to convert the bubble rise velocity to bubble size for each group of bubbles.

References

Abou-el-Hassan, M. E., "A generalized bubble rise velocity correlation," *Chem. Eng. Commun.*, **22**, 243 (1983).

Daly, D. G., S. A. Patel, and D. B. Bukur, "Measurement of gas holdups and Sauter mean bubble diameters in bubble column reactors by dynamic gas disengagement method," *Chem. Eng. Sci.*, **47**, 3647 (1992).

Fan, L.-S. and K. Tsuchiya, *Bubble Wake Dynamics in Liquids and Liquid-Solid Suspensions*, Butterworth-Heinemann, Stoneham, MA, 43 (1990).

Peebles, F. N., and H. J. Garber, "Studies on the motion of gas bubbles in liquids," *Chem. Eng. Prog.*, **49**, 88 (1953).

Marrucci, G., "Rising velocity of a swarm of spherical bubbles," *Ind. Eng. Chem. Fund.*, 4, 224 (1965).

Clift, R., J. R. Grace, and M. E. Weber, *Bubbles Drops and Particles*, Academic Press, New York, 171, 236 (1978).

Notations

P	Pressure
z	Distance from the distributor
g	Gravitational constant
K	Constant defined in Eq. (3)
H	Bed height
t	Time
t_0	Time of gas shut-off
U_b	Bubble rise velocity
d_b	Bubble size
A	Cross-sectional area of the column
U_t	Particle terminal velocity
Mo	Morton number of liquids
d_e	Volume equivalent diameter of bubbles

Greek

ρ	Density
ε	Holdup
μ	Viscosity
ϕ	Shape factor of particles

Subscripts

g	Gas phase
l	Liquid phase
s	Solid phase
m	Liquid-solid medium

Superscript

0	Gas-free liquid-solid suspension

Table 1. Bubble Rise Velocities and Holdups of Various Bubbles Groups (U_g = 32.4 cm/s)

i	t_i (s)	$\varepsilon_g(t_i)$	S_i	U_{bi} (m/s)	$\varepsilon_{g0,i}$
0	1.64	0.43			
1	2.05	0.245	-0.451	0.84	0.068
2	2.54	0.105	-0.286	0.38	0.181
3	3.25	0.045	-0.0845	0.21	0.120
4	6.03	0.018	-0.00971	0.079	0.022
5	10.02	0	-0.00451	0.041	0.038

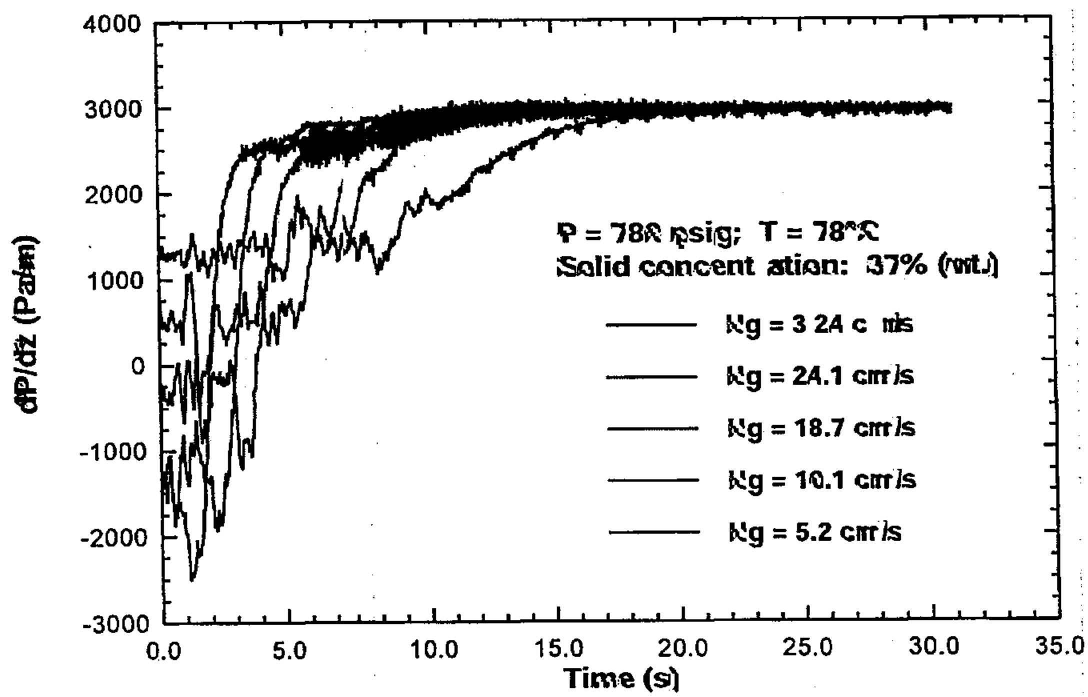

Figure 1. Dynamic Pressure Drop Signals in Bed Collapse Processes at Various Gas Velocities

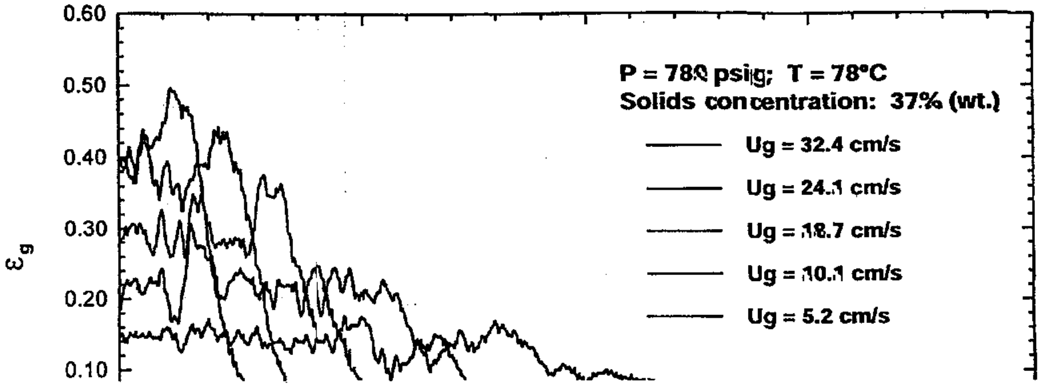

P = 780 psig; T = 78°C
Solids concentration: 37% (wt.)
Ug = 32.4 cm/s
Ug = 24.1 cm/s
Ug = 18.7 cm/s
Ug = 10.1 cm/s
Ug = 5.2 cm/s
0.60
0.50
0.40
0.30
0.20
0.10
ε_g

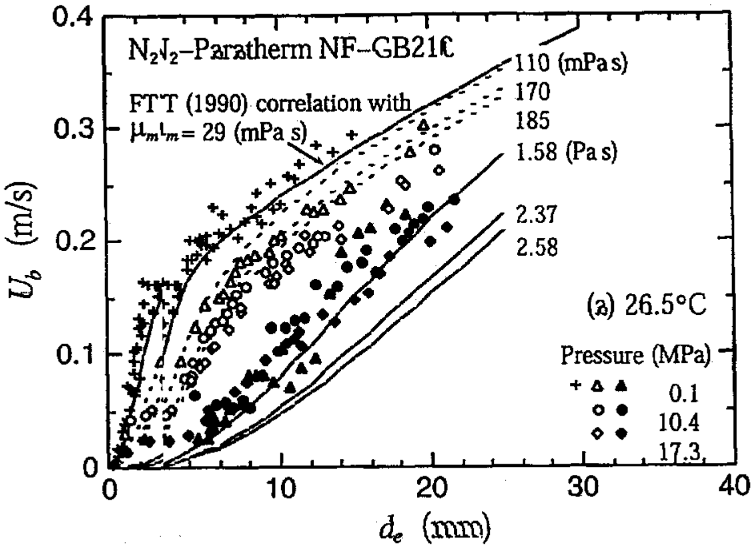
N2-Paratherm NF-GB21C
FTT (1990) correlation with
110 (mPa s)
170
185
1.58 (Pa s)
2.37
2.58
(a) 26.5°C
Pressure (MPa)
0.1
10.4
17.3
0.4
0.3
0.2
0.1
0
0
10
20
30
40
U_b (m/s)
d_e (mm)

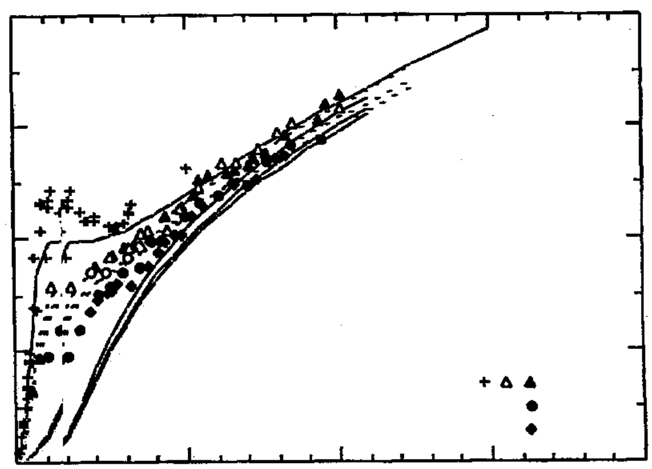

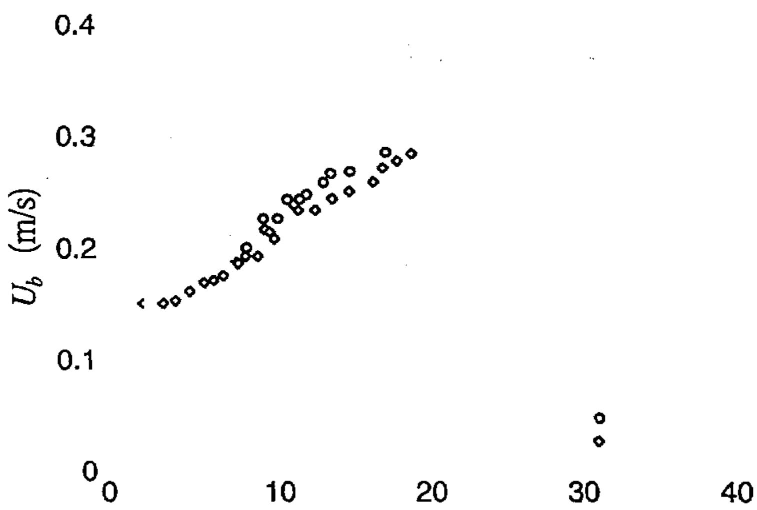
0.4
0.3
0.2
0.1
0
U_b (m/s)
0
10
20
30
40

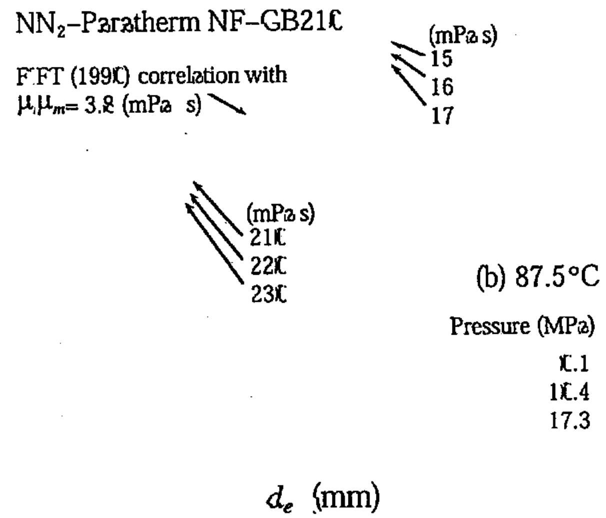

Figure 4. Comparison beetween the predictions and the experimental data, under high pressure conditions (Sololids holdups for +, open, and filled symbols are 0, 0.381 and 0.555, respectively; lirines: predictions).